Pharm Res (2015) 32:3756–3767
DOI 10.1007/s11095-015-1737-8

RESEARCH PAPER

Polymeric Micelles of PEG-PLA Copolymer as a Carrier for Salinomycin Against Gemcitabine-Resistant Pancreatic Cancer

Zahra Daman[1] • Hamed Montazeri[2] • Masoumeh Azizi[3] • Faegheh Rezaie[3] • Seyed Nasser Ostad[4] • Mohsen Amini[5] • Kambiz Gilani[1,6]

Received: 15 February 2015 / Accepted: 8 June 2015 / Published online: 31 July 2015

ABSTRACT

Purpose Resistance to gemcitabine in pancreatic cancer (PC) may account for the failure of conventional treatments. Recently, salinomycin (SAL) has been identified as selective inhibitor of cancer stem cells (CSCs). In our study, we aimed to deliver SAL to gemcitabine-resistant PC by the aid of poly ethylene glycol-b-poly lactic acid (PEG-b-PLA) polymeric micelles (PMs).

Methods SAL-loaded PMs were prepared and investigated in terms of pharmaceutical properties. MTT and Annexin V/PI assays were used to study cell proliferation and apoptosis in AsPC-1 cells in response to treatment with SAL micellar formulations. Alterations in CSC phenotype, invasion strength, and mRNA expression of epithelial mesenchymal transition (EMT) markers were also determined in the treated cells. *In vivo* antitumor study was performed in Balb/c AsPC-1 xenograft mice.

Results PM formulations of SAL were prepared in suitable size and loading traits. In gemcitabine-resistant AsPC-1 cells, SAL was found to significantly increase cell mortality and apoptosis. It was also observed that SAL micellar formulations inhibited invasion and harnessed EMT in spite of induced expression of Snail. The *in vivo* antitumor experiment showed significant tumor eradication and the highest survival probability in mice treated with SAL PMs.

Conclusions The obtained results showed the efficacy of SAL nano-formulation against PC tumor cells.

KEY WORDS cancer stem cells · epithelial mesenchymal transition · pancreatic cancer · polymeric micelles · salinomycin

ABBREVIATIONS

CMC	Critical micelle concentration
CSCs	Cancer stem cells
DLS	Dynamic light scattering
EE	Entrapment efficiency
EMT	Epithelial to mesenchymal transition
EPR	Enhanced permeability and retention
FBS	Fetal bovine serum
HPLC	High performance liquid chromatography
$IC_{50\%}$	50% inhibitory concentration
LD	Loading density
MTT	3-(4,5-dimethylthiazolyl-2)-2,5-diphenyl tetrazolium bromide
NP	Nanoparticle
PBS	Phosphate buffered saline
PC	Pancreatic cancer
PDI	Polydispersity index
PEG-b-PLA	Poly ethylene glycol-b-poly lactic acid
PI	Propidium iodide
PMs	Polymeric micelles
RT-PCR	Real-time polymerase chain reaction
SAL	Salinomycin

✉ Kambiz Gilani
gilani@tums.ac.ir

[1] Aerosol Research Laboratory, Department of Pharmaceutics, School of Pharmacy, Tehran University of Medical Sciences, Tehran, Iran

[2] Department of Molecular Biology, Pasteur Institute of Iran, Tehran, Iran

[3] Biotechnology Research Center, Pasteur Institute of Iran, Tehran, Iran

[4] Department of Toxicology-Pharmacology, School of Pharmacy, Tehran University of Medical Sciences, Tehran, Iran

[5] Department of Medicinal Chemistry, School of Pharmacy, Tehran University of Medical Sciences, Tehran, Iran

[6] Medicinal Plants Research Center, Tehran University of Medical Sciences, Tehran, Iran

TEM	Transmission electron microscopy
THF	Tetrahydrofuran

INTRODUCTION

Pancreatic cancer (PC) is one the most lethal tumors worldwide which is characterized by insidious onset, late diagnosis and low survival rate (1). The median survival rate in these patients is only 6 months after the clinical diagnosis and the 5-year survival rate is less than 6%, which has been remained unchanged over the last decades (2). Currently, most of the chemotherapy regimens use gemcitabine as the drug of choice for the treatment of PC (3). However, patients generally show limited response to gemcitabine because of the serious drawbacks associated with this drug including rapid body clearance (4), which leads to significant dose-related side effects, and intrinsic or extrinsic drug resistance in tumor cells (5).

On the way toward finding new therapeutic strategies for optimal treatment of cancer, various studies have identified a subset of cancer cells within different types of solid tumors including PC, termed as cancer stem cells (CSCs), which play critical role in tumor invasiveness, metastasis, and recurrence (6). Importantly, CSCs show noticeable drug and radioresistance characteristics, which leads to enrichment of this population in some tumors after being treated by conventional cancer therapies (7). Thus, a failure of eradicating CSCs in tumors makes it more likely that these cells survive and spread to distant sites. On the other hand, it has been shown that the process of epithelial to mesenchymal transition (EMT) during which cell dissociation occurs, contributes to the aggressiveness of pancreatic cancer cells (8). While EMT is a normal physiological phenomenon throughout the embryonic development and tissue reconstruction, it is also an important promoter of tumor migration/metastasis as well as drug resistance in certain cancer cells (9). Recently, it has been suggested that CSCs and EMT-type cells share many molecular characteristics with each other and thus have become novel therapeutic targets for successful treatment of tumor persistence and progression (7). In this regard, in a high-throughput screening study in 2009, Gupta *et al.* identified a selective agent, salinomycin (SAL) that showed increased activity against EMT-induced breast CSCs (10). SAL is a polyether antibiotic that has been originally used as an anticoccidial drug in poultry for more than 30 years and is also fed in livestock to improve nutrient absorption (11). Recently, several studies have demonstrated that SAL is not only capable of targeting CSCs in different types of cancer cells, but also can eradicate regular tumor cells as well as highly resistant ones (11). In particular, previous study by Zhang *et al.* showed that SAL could inhibit the $CD133^+$ pancreatic CSCs along with $CD133^-$ non-CSCs (12).

Based on these findings, SAL may be a promising candidate for future anti PC treatments. However, it represents important limitations toward effective clinical applications such as poor aqueous solubility and off-target toxicity. Incorporation of SAL into nanoparticle (NP) carriers can address these predicaments. Recently, iTEP-based SAL NPs were shown to improve the tumor accumulation of drug and boost the CSC elimination in murine breast cancer 4 T1 orthotopic model (13). However, these NPs could not efficiently inhibit the tumor growth and their therapeutic outcome was statistically indifferent from free SAL treatment.

One possible reason for the aforementioned marginal antitumor effect of SAL NPs may be that the iTEP carrier lacks stable enough encapsulation of SAL. Thus here, we aimed to develop a polymeric micelle (PM) formulation of SAL as a potential therapy for PC. In fact, PMs offer certain advantages as anticancer drug delivery vehicles including drug solubilization, high stability, sustained drug release, prolonged *in vivo* circulation, passive tumor targeting through the enhanced permeability and retention of the nanomedicine (EPR effect), and decreased drug toxicity (14). In the present study, we applied the FDA-approved poly ethylene glycol-b-poly lactic acid (PEG-b-PLA) block copolymer for the construction of SAL-loaded micelles. This copolymer has shown immense safety and efficacy in numerous experimental formulations including Genexol®-PM, a micelle formulation of paclitaxel, which was approved in Korea at 2007 and is currently under clinical development in the USA (15). This formulation holds the chief advantages of significantly improved maximum tolerated dose in humans compared to Taxol® and the absence of Cremophor EL and its side effects (16). Our SAL-loaded PEG-PLA micelles were prepared by applying two different fabrication methods and compared to each other in terms of size, zeta potential and loading properties. In the next step, the morphology, release behavior and cytotoxicity of the selected formulations were investigated. Human pancreas cancer AsPC-1 cells were chosen as the model for cancer cells because they were demonstrated to be highly resistant to gemcitabine (17). The *in vivo* antitumor activity in balb/c mice bearing AsPC-1 cancer xenogafts was also evaluated. Additionally, we aimed to extend our understanding of the effects of SAL-loaded PMs on induction of apoptosis, CD133 expression and EMT.

MATERIALS AND METHODS

Gemcitabine and SAL were purchased from Hangzhou Dayangchem Co. Ltd. (Hangzhou, China). mPEG(2 k)–PLA(2 k) (Mw/Mn = 1.11) was supplied from Advanced Polymer Materials Inc. (Montreal, Canada). 3-(4,5-dimethylthiazolyl-2)-2,5-diphenyl tetrazolium bromide

(MTT) was purchased from Sigma–Aldrich (St. Louis, MO, USA). HPLC-grade tetrahydrofuran (THF) and methanol were from Duksan Pure Chemical Co. (Korea). The rest of solvents and chemicals were of analytical grade and supplied locally. Human pancreatic cancer AsPC-1 cells and murine fibroblast NIH/3 T3 cells were obtained from Pasteur Institute (Tehran, Iran) and grown in RPMI 1640 medium supplemented with 10% fetal bovine serum (FBS), 100 U/mL of penicillin, and 100 mg/mL of streptomycin, all from Biosera (UK).

Preparation of SAL-Loaded Micelles

SAL solubilized in PEG-PLA micelles was prepared by the two following techniques:

(A) The well-established nanoprecipitation process, consisted of the following steps, weighing of SAL (1 or 2 mg) and the polymer (20 mg) into a glass vial, dissolving in 1 mL THF, addition of subsequent organic phase to 10 mL water under probe sonication using a Hielscher device (model UP400S, Hielscher ultrasound technology, Germany) at 50% power for 2 min, and removal of THF by a rotary evaporator (Buchi Rotavapor R-124, Buchi, Switzerland).

(B) The film hydration method was performed as follows. 1 or 2 mg SAL and 20 mg PEG-b-PLA were dissolved in 2 mL THF. The organic solvent was then removed by the rotary evaporator to form a thin film of the drug and the polymer. This film was further dried under high vacuum for 2 h to remove any remaining traces of the solvent. Drug-loaded micelles were formed by resuspending the film in 10 mL deionized water under stirring at 30°C for 30 min, followed by a sonication for 5 min to reach the room temperature.

Blank micelles were prepared according to the same protocols in the absence of SAL, while keeping the same polymer concentration at 2 mg/mL to allow comparisons between unloaded and loaded samples.

Micelle Size and Zeta Potential

The micelle size (hydrodynamic diameter) and zeta potential were measured by the dynamic light scattering (DLS) instrument using a Zetasizer Nano (Malvern instruments Ltd., UK). Scattered light was detected at 25°C at an angle of 90°. The particle size distribution (PDI—polydispersity index) of all samples was measured in triplicate with 16 runs each, while the zeta potentials were acquired based on 100 measurements for each sample in 0.01 M PBS (PH 7.4).

Quantification of SAL

SAL cannot be determined by direct spectrophotometric methods because it does not possess any significant UV absorbance activity. Thus, pre-column derivatization with 2,4-dinitrophenyl-hydrazine was used in order to improve its detection according to previously established method (18).

The high performance liquid chromatography (HPLC) system consisted of the following: a 600E HPLC system equipped with a UV detector (Water, Millipore, USA) and a C18 column (150 mm × 4.6 mm, Optimal ODS—H, Capital HPLC, UK). The mobile phase was composed of methanol and 1.5% aqueous acetic acid (95:5 *v/v*) and was delivered at a flow rate of 1.0 mL/min in all experiments. The detection was performed at the wavelength of 392 nm. All samples were analyzed in triplicate. The generated calibration curve covered the concentration range from 1 to 100 μg/mL.

Loading Characteristics and Solubility Study

Five milliliter of the SAL-loaded micellar solution was centrifuged at a rotational speed of 6000 RPM for 10 min at 4°C using Amicon Ultra Centrifugal Filter Devices (MW cutoff = 10 kDa). The content of free SAL in the resulting supernatant was measured according to the aforementioned HPLC method. The total amount of SAL in the system (free and micelle encapsulated) was then determined by freeze drying of the micellar aqueous dispersion and diluting the dried powder with methanol prior to applying onto pre-column derivatization procedure.

The entrapment efficiency (EE) and loading density (LD) were calculated as follows:

$$\begin{aligned} \mathrm{EE}(\%\,\mathrm{w/w}) &= (\text{amount of loaded SAL/Total amount of SAL used for loading}) \times 100 \mathrm{LD}(\%\,\mathrm{w/w}) \\ &= (\text{amount of loaded SAL/total amount of the drug and copolymer used for loading}) \times 100 \end{aligned}$$

The solubility of SAL-loaded micelles (*w/v*) is defined as the amount of loaded SAL per unit volume of water. In addition, the solubility of free SAL in deionized water was determined by adding an excess amount of SAL to 10 mL of water. The mixture was stirred at 37°C for 1 h. Then, the mixture was filtered through a 0.45-μm filter to remove insoluble SAL.

The amount of soluble SAL was measured by HPLC as described in the assay section above.

Transmission Electron Microscopy (TEM)

Morphological characteristics of the SAL-loaded micelles were examined using a TEM machine (Zeiss, EM10C 80 kV, Germany). Briefly, samples were deposited on the carbon-coated copper grids and examined through TEM after being dried at the room temperature.

Drug Release from PEG-PLA Micelles

In vitro release kinetics of SAL from PMs was carried out by a dialysis method, while using 0.01 M phosphate buffered saline (PBS) containing 0.5% SDS (pH 7.4) as the dissolution medium. In fact, the surfactant was added to the medium in order to guarantee sink conditions for the complete release period. Briefly, a sample of drug loaded micelles in pure water (2 mL, 350 μg SAL) was introduced into a dialysis membrane bag (Mw cut-off = 8 kDa, Spectrum laboratories, USA), immersed in 20 mL dissolution medium, and incubated at 37°C under mild stirring rate of 100 rpm. Medium aliquots were withdrawn from the beaker and replaced with equal volume of it at predefined time points. Finally, the lyophilized samples were diluted with methanol to estimate the amount of drug released from the PMs by RP-HPLC, as described above. The release tests were performed in triplicate.

Cytotoxicity Assay

Human pancreatic cancer (AsPC-1) and normal mouse fibroblast (NIH/3 T3) cell lines were plated at 10^4 cells per well density in 96-well plates and incubated overnight at 37°C and 5% CO2. Afterwards, the medium was replaced with fresh medium containing either free drug solution in DMSO (less than 2% *v/v*) or SAL-loaded PMs with drug concentrations ranging from 0 to 25 μM. Untreated or DMSO-treated cells were served as controls for the experiments. After 48 h, the cell survival was determined using MTT assay. Briefly, 20 μL of MTT reagent (5 mg/mL, Sigma) was added to the wells followed by incubation for 4 h at 37°C. Later, 100 μL of DMSO was added to dissolve the insoluble purple formazan product. At the end, the absorbance of the reduced MTT was measured at 570 nm with 690 nm as a reference readout using a microplate reader (Bio-Rad, Model 680, USA). The percentage of the absorbance present in drug treated cells compared to that in the control cells was calculated. IC_{50} values (The 50% inhibitory concentrations) were determined from dose–response curves by a nonlinear regression analysis using the GraphPad Prism 5.0 (GraphPad Software, Inc., La Jolla, CA, USA).

Annexin-V/Propidium Iodide (PI) Apoptosis Assay

The measurement of apoptosis in AsPC-1 tumor cells was done using an Annexin V-FITC Apoptosis Detection Kit (BD Biosciences, San Jose, CA, USA). Briefly, apoptosis was induced in 10^6 cells by incubation with SAL-loaded PMs (4 and 8 μM) for 24 and 48 h. Afterwards, the cells were harvested, washed with cold PBS, and resuspended in 100 μl of Annexin V (1×) binding buffer. Annexin V and PI double staining was performed according to the prescribed protocol. The labled cells were incubated at room temperature in the dark for 15 min, and diluted with 400 μl binding buffer prior to flowcytometry analysis using FACSCalibur (Becton-Dickinson, Heidelberg, Germany) and the Cell Quest software. The early apoptotic cells were determined by calculating the percentage of Annexin V+/PI- AsPC-1 populations, while Annexin V+/PI+ fraction was considered as late apoptotic cells.

Flow Cytometric Analysis of Pancreas Cancer AsPC-1 Cells

To measure the inhibitory effect of SAL-loaded PMs on CD133+ population, the AsPC-1 cells were seeded into 6-well plates at 10^6 cells/well and grown at 37°C and 5% CO_2 for 24 h. Then, the cells were treated with SAL-loaded micelles diluted with complete medium at the $IC_{50\%}$ concentration for 48 h. The blank culture medium was used as the control. After incubation, the harvested cells were stained with anti-C133-PE antibody (ebioscience, San Diego, CA, USA) in accordance with the manufacturer's protocol at 4°C for 20 min in PBS. PE-conjugated antibody against mouse IgG1 (ebioscience) was used as isotype control. The expression of CD133+ marker was evaluated by using a FACSCalibur flowcytometer.

Scratch Migration Assay

Monolayer cells grown to confluence in 6 well plate, were scratched using a 100 μl pipette tip, to generate a "wound" *in vitro*. Cells were then washed with PBS and medium was replaced by fresh medium containing 2, 4 and 8 μM of SAL. After 24 and 48 h, treated cells were examined under an Olympus IX71 inverted microscope (Olympus Corporation, Tokyo, Japan), and the distance between two edges of wound was estimated using OLYSIA BioReport® software (Olympus, Tokyo, Japan). Wound closure rate was determined according to the following equation:

$$\%\text{wound closure} = (\text{initial wound width} - \text{wound width 48h of post treatment})/\text{initial wound width} \times 100.$$

Quantitative Real-Time Polymerase Chain Reaction (RT-PCR)

Total RNA was isolated from AsPC-1 cells after treatment with SAL-loaded PMs ($IC_{50\%}$) using TriPure® isolation reagent (Roche Applied Science) according to the manufacturer's protocol. RNA concentration was quantified by a spectrophotometer (IMPLEN, Germany), and RNA quality was assessed by determining the A260/A280 ratio. cDNA was synthesized from 1 μg of total mRNA using M-MuLV reverse transcriptase enzyme (Fermentas, St Leon-Rot, Germany) according to the manufacturer's recommendations. Negative controls tubes containing no cDNA were also prepared separately for each gene. In the next step, 1 to 2 μL of diluted transcription products were used for RT-PCR. The reactions were performed in a volume of 25 μL containing 140 ng of specific primers and 12.5 μL SYBR green master mix (Takara Biotechnology, Dalian, china) in the following condition:

Initial denaturing: 95°C for 10 min, followed by 40 cycles of denaturing at 95°C for 30 s, annealing at 59°C for 40 s, and extension at 72°C for 30 s. Statistical analysis for relative mRNA expression was performed by REST proposed by *Pfaffl* (19) and beta actin was used as an internal reference gene.

Primers for RT-PCR were designed using AlleleID 6 software. To determine the specificity of each primer BLAST was carried out using NCBI Nucleotide software (http://blast.ncbi.nlm.nih.gov/) and synthesized by Metabion intentional AG (Martinstied/Lena-Christ-Strasse, Deutshland, Germany). The following sequences were used:

CDH1 Forward: TAATTCTGATTCTGCTGCTC TTGC
CDH1 Reverse: TCAAAGTCCTGGTCCTCTTCTCC
SNAI1 Forward: GGTTCTTCTGCGCTACTGCTG
SNAI1 Reverse: GCTGCTGGAAGGTAAACTCTGG
VIM Forward: GGCGAGGAGAGCAGGATTTC
VIM Reverse: CAACCGTCTTAATCAGAAGTGTCC
ZEB-1 Forward: GAAGATAACTTTAGTTGCTCCC TGTG
ZEB-1 Reverse: TGAATTTACGATTACACCCAGA CTG

In Vivo Treatment

All the care and handling of animals were conducted in accordance with guidelines approved by the Animal Care Committee of Tehran University of Medical sciences.

The antitumor activity of free SAL and SAL-loaded PMs were evaluated in Balb/c mice bearing subcutaneous AsPC-1 tumor. Six days after inoculation (2×10^6 cells/mouse), mice were administered intraperitoneally every other day with saline, blank micelles, SAL-loaded PMs, and free SAL solution (in <10% ethanol) over 4 weeks at a dose equivalent to 5 mg/kg SAL. At the same time, an additional group of six mice was treated weekly with gemcitabine solution (100 mg/kg) in order to assess the efficacy of standard treatment for pancreatic cancer. Meanwhile, the tumor volume, animals body weight, and the overall morbidity were closely monitored. The tumor volume was measured by the aid of a digital vernier caliper through the following equation: $V = ½ [a \times b^2]$ where a and b are the longest and the shortest diameters, respectively.

Statistics

All results were presented as mean ± SD. Data from various formulations were compared using one-way or two-way ANOVA. A p value less than 0.05 was considered to be statistically significant.

RESULTS

Preparation and Characterization of SAL-Incorporated PEG-PLA Micelles

The film hydration and solvent evaporation methods were investigated for the preparation of SAL-loaded as well as unloaded PEG-PLA micelles. The feed drug to polymer (% *w/w*) ratios used for preparation of PMs were 5% and 10% for both methods. For all formulations, more than 85% of the initial amount of the drug was incorporated into the micelles. In this regard, neither the preparation method, nor the drug concentration, did alter the EE of SAL into PEG-PLA micelles ($p>0.05$). Hence, using a higher initial drug amount, the loading density increased accordingly within both groups (Table I).

The sizes of blank and drug-loaded micelles were determined utilizing DLS for each of the fabrication methods examined (Fig. 1a). The blank and drug-loaded samples were analyzed without dilution and filtration steps in order to avoid any loss of the particles. The Z-average sizes of drug-free micelles were 32.13 ± 6.46 nm and 42.13 ± 6.54 nm in film

Table I Loading Properties of SAL-Loaded PMs Prepared from Different Fabrication Methods

Fabrication method	Initial drug to polymer ratio (%)	Encapsulation efficiency (%)	Loading density (%)
Nanoprecipitation	5	90.2 ± 2.6	4.8 ± 0.1
	10	88.4 ± 2.2	8.7 ± 0.4
Film hydration	5	89.8 ± 3.4	4.8 ± 0.2
	10	85.6 ± 2.3	8.3 ± 0.4

Mean ± SD, $n = 3$

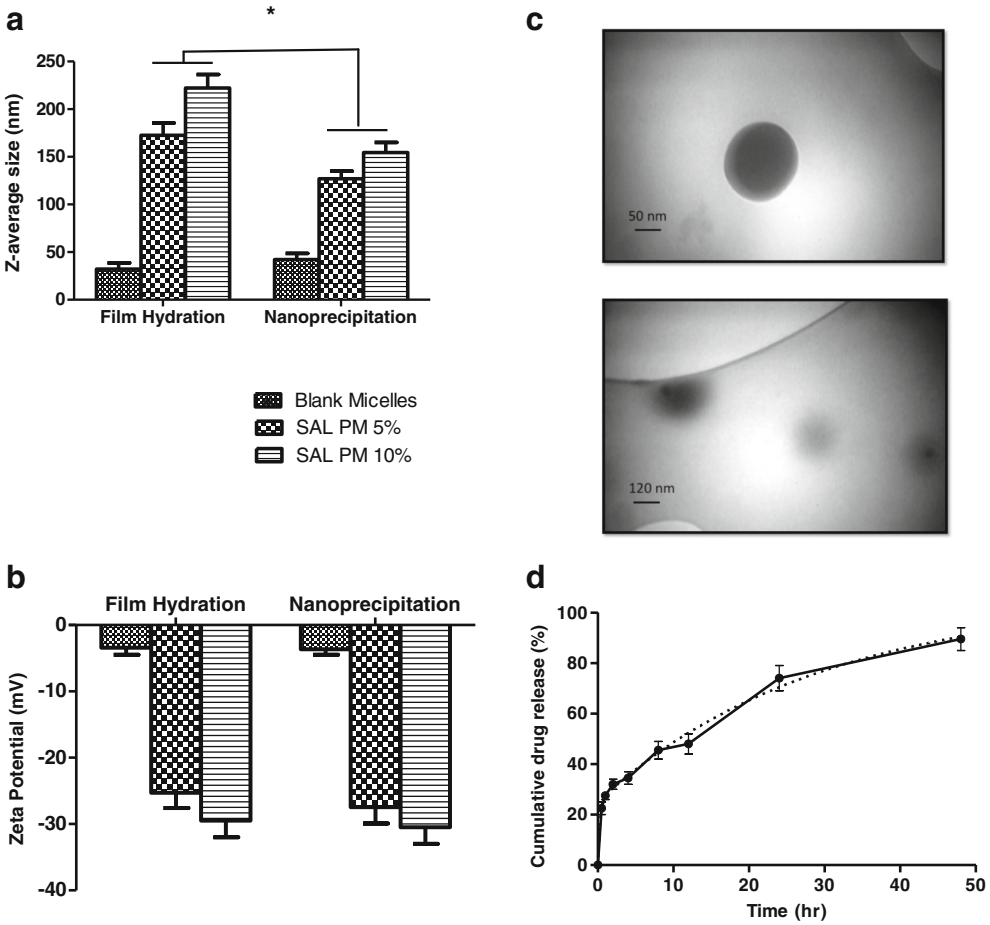

Fig. 1 Physicochemical characterization of SAL-loaded micelles (**a**) Hydrodynamic size of blank and drug-loaded PEG-b-PLA micelles prepared by different methods, * indicates $P < 0.05$ (**b**) Surface zeta potential of blank and drug-loaded PEG-b-PLA micelles (**c**) Transmission electron micrographs of SAL-loaded polymeric micelles (**d**) The *in vitro* release behavior of SAL (10% *w/w*) from PEG-b-PLA micelles in pH 7.4.

hydration and nanoprecipitation methods, respectively. The drug incorporation was accompanied by an increase in both particle size and negative zeta potential. The higher drug loading ratios induced larger particle diameters. The nanoprecipitation technique yielded micelles with smaller diameters compared to the film hydration method, with the Z-average sizes of 154.5±10.6 nm at 10% *w/w* and 127.1± 7.7 nm at 5% *w/w* drug to polymer ratios. As demonstrated in Fig. 1b, the surface charge of the SAL-loaded PMS was independent from the preparation method. Considering favorable particle size and appropriate loading characteristics, the 10% (*w/w*) SAL-loaded micelles which were produced by nanoprecipitation procedure were chosen as the optimal formulation for further *in vitro* and *in vivo* studies. The particle size and morphology of the selected formulation, referred to as SAL PM 10%, was further investigated by TEM. These SAL-loaded micelles exhibited uniform spherical shape, with the size in agreement with that measured by the DLS technique (Fig. 1c). It should be also mentioned that due to high logP value (5.15) of SAL, its aqueous solubility is very low (1.7 μg/mL). However, its solubility reached to 200 μg/mL by the use of PEG-PLA micelles in SAL PM 10% formulation.

In Vitro Release of SAL from PEG-PLA Micelles

The release rate of SAL from PEG–PLA PMs was examined *in vitro* and is shown in Fig. 1d. We used 0.5% *w/v* SDS as a solubilizer in the release medium (PH 7.4 PBS buffer at 37°C) to provide the sink condition during the study. The release curve indicates that about 20% of the drug released within the initial stage, after which the release rate shifted to a sustained stage with the most of drug (≈90%) being released over the course of 2 days. Additionally, simulated drug release curve was generated using two phase exponential association (GraphPad Prism), and was significantly fitted on the experimentally measured cumulative release data. The derived rate constants for the fast and sustained phases were used to calculate the $t_{1/2}$ of the SAL release from PEG-PLA micelles. The goodness of fit and the resultant data are presented in Table II.

In Vitro Cytotoxicity of SAL-Loaded Micelles

Figure 2 depicts *in vitro* relative inhibitory rate of AsPC-1 pancreas tumor cell line and NIH3T3 mouse fibroblasts after 48 h of incubation with free SAL solution in DMSO (<2% *v/v*), and SAL PM 5% and 10% at different drug

Table II Curve Fitting Parameters of *In Vitro* SAL Release from PEG-PLA PMs

K[a] fast (h^{-1})	K slow (h^{-1})	Fast half life (h)	Slow half life (h)	Goodness of fit (R^2)
3.728	0.034	0.186	20.31	0.978

Mean ± SD, $n = 3$

[a] K stands for rate constant

doses. The MTT assay was performed to measure the changes in cell proliferation and viability following drug treatment. The AsPC-1 cells experienced noticeable toxicity towards SAL formulations in a dose dependent manner, while we had previously demonstrated that they are highly resistant to gemcitabine in a wide range of doses from 1 to 100 μM (17). As shown in Table III, the IC_{50} of SAL solution (7.99 ± 0.35 μM) was lower than that of SAL PM 5% and 10%, but this difference was not statistically significant. Importantly, the blank PEG-PLA micelles were shown to have no noticeable cytotoxicity on tumor cells at a concentration range equivalent to 5% and 10% SAL loading. In a parallel experiment, NIH3T3 cells also exhibited noticeable sensitivity to SAL treatment with higher IC_{50} values than the cancerous cells ($p < 0.05$). However, it was found that free SAL and SAL-loaded PMs had less

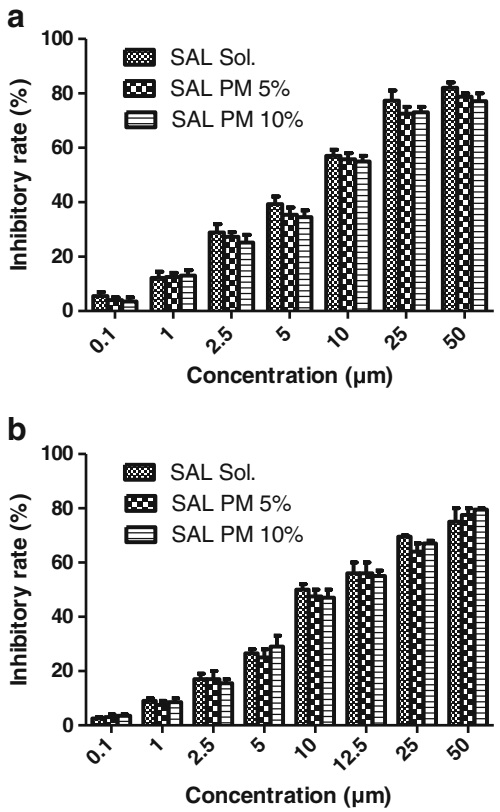

Fig. 2 *In vitro* inhibitory effects of free SAL and SAL-loaded micelles on (**a**) AsPC-1 cells and (**b**) NIH3T3 cells for 48 h.

Table III $IC_{50\%}$ (μM) values of free SAL solution and SAL-loaded PMs

Sample	$IC_{50\%}$ (μM) in cell line	
	AsPC-1	NIH3T3
Free SAL solution	7.99 ± 0.35	9.01 ± 0.48
SAL PM 5%	8.66 ± 0.51	9.12 ± 0.67
SAL PM 10%	8.97 ± 0.42	9.72 ± 0.59

(Mean ± SD, $n = 5$)

cytotoxic effect on the normal NIH3T3 cells than cancerous AsPC-1 cells in concentrations up to 5 μM SAL. Similarly, no considerable toxicity was found by the empty PEG-PLA micelles on NIH3T3 cells.

Flow Cytometric Analysis of AsPC-1 Cells

Figure 3a shows enhanced apoptosis in case of AsPC-1 cells treated with SAL-loaded PMs in a time and dose dependent manner. At 24 h, the SAL treated cells showed a subpopulation of cells in apoptosis in either early stage (Annexin+ /PI-) or late stage (Annexin+ /PI+) of programmed cell death. At this initial period of incubation, the lowest cell populations belonged to necrotic cells. However, after 48 h of incubation, 8 μM SAL PM induced necrosis (Annexin- /PI+) in 34.9% of cells, while treatment with 4 μM SAL PM led to necrosis of 15.7% of cells ($p < 0.05$).

To further investigate that SAL-loaded PMs have additional toxicity on CD133+ cells, a flow cytometry study was conducted to assay the proportion of CD133+ CSCs in 48 h treated AsPC-1 cells. Our results presented in Fig. 3b showed that SAL nano formulation treatment changed the proportion of CD133+ cells from 14.84% to 12.36%, although not reaching the statistical significance ($p > 0.05$).

Scratch Migration Assay

The strength of invasion is one of the key features of cancer cells, which is often activated by EMT. In this regard, we sought to interrogate invasive properties of AsPC-1 cells in presence of SAL micellar formulation by the aid of scratch migration assay. This experiment showed that SAL treatment at concentrations of 2, 4, and 8 μM decreased migratory abilities of AsPC-1 cell line in 24 and 48 h after scratching (Fig. 4a, b), consistent with the notion that SAL harnesses invasiveness of cancerous cells.

RT-PCR Analysis

To gain insights into the mechanism of SAL effects on highly metastatic AsPC-1 cells, we examined any changes in expression

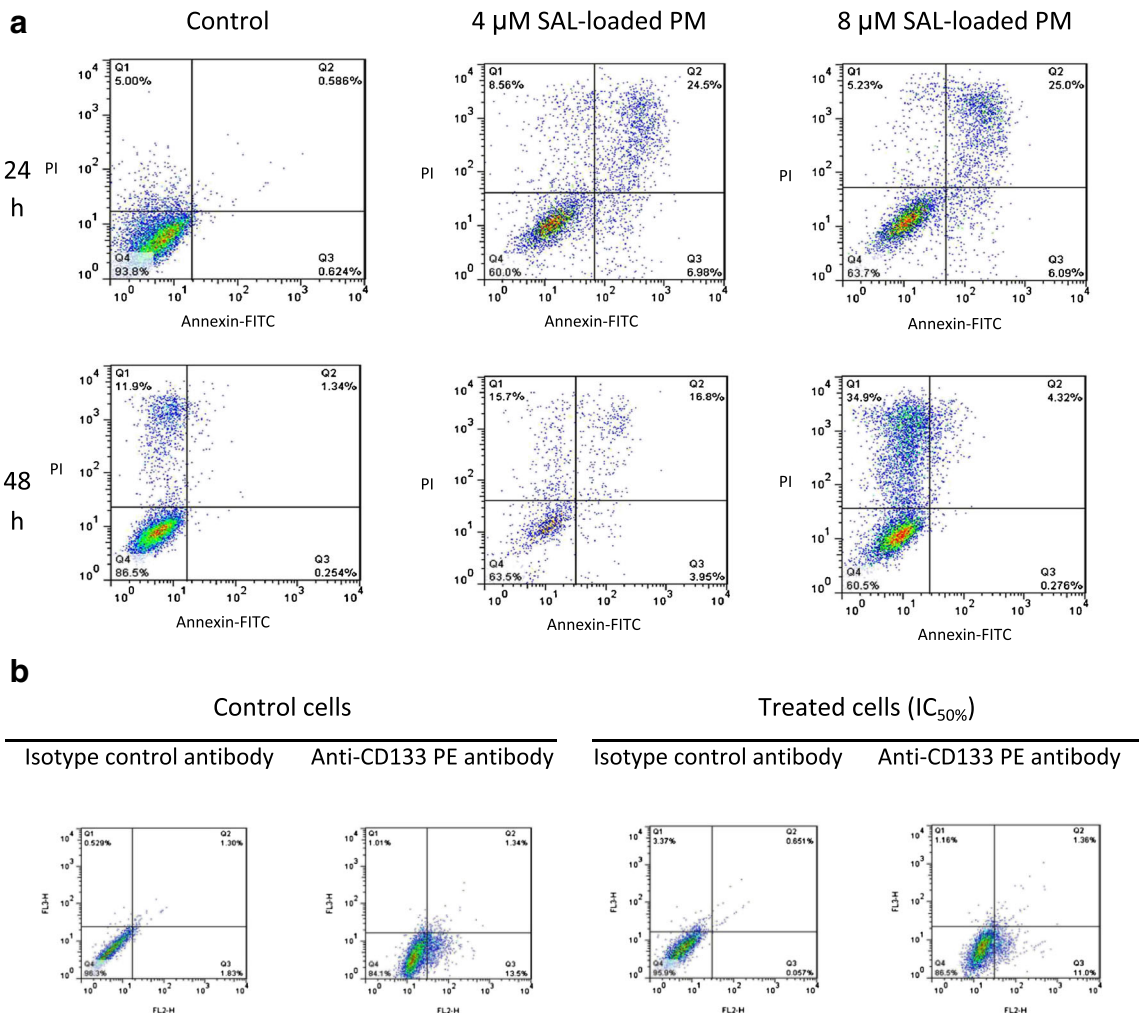

Fig. 3 (**a**) Annexin V-FITC/PI double staining analysis of apoptosis in AsPC-1 cells treated with SAL-loaded polymeric micelles (**b**) flow cytometric analysis of CD133 expression in AsPC-1 cells after treatment with SAL-loaded PEG-PLA micelles.

of E-cadherin (CDH1), Snail (SNAI1), VIM and ZEB-1 as major regulatory markers of EMT using quantitative RT-PCR (Fig. 4c). The results revealed that relative to the mRNA expression in untreated cells, the level of E-cadherin mRNA in treated cells decreased by 3.58 fold, while expression of mRNA encoding SNAI1 increased by 8.87 fold in response to 48 h exposure with $IC_{50\%}$ dose of SAL micellar formulation ($p<0.001$). On the other hand, VIM and ZEB-1 expression decreased drastically by the factor of 2.45 and 2.23, respectively ($p<0.001$).

In Vivo Therapeutic Efficacy

AsPC-1-tumor bearing mice were randomly divided in four groups and injected intraperitoneally with PBS (as control), SAL solution, and SAL PM 10% for every other day, and with conventional gemcitabine solution for once a week. The treatment duration for all mice groups were over 4 weeks. As seen in Fig. 5a, the tumor size of mice injected with PBS grew aggressively and reached the volume of almost 1000 mm^3, 28 days after inoculation. However, our results showed that both SAL solution and SAL PM 10% were able to abolish tumors significantly compared to the PBS-treated control after 28 days treatment course. The tumor size reduction that was achieved by SAL PM 10% was not statistically different from that of SAL solution ($p<0.05$). The antitumor effect was also observed in mice that were injected weekly with high-dose gemcitabine solution. However, the latter treatment could not decrease the initial tumor size, but only inhibited further tumor growth. Moreover, the body weight of gemcitabine-treated mice decreased considerably during the study period, while no significant body weight alteration was observed in mice treated either with free SAL solution or with SAL micelle formulation (Fig. 5b). As displayed in Fig. 5c, the survival probability for SAL-loaded PMs and free SAL solution were 100% and 66.7%, respectively, over the period of 40 days. The median survival time for gemcitabine-treated mice was 21 days compared to 35 days in the control group.

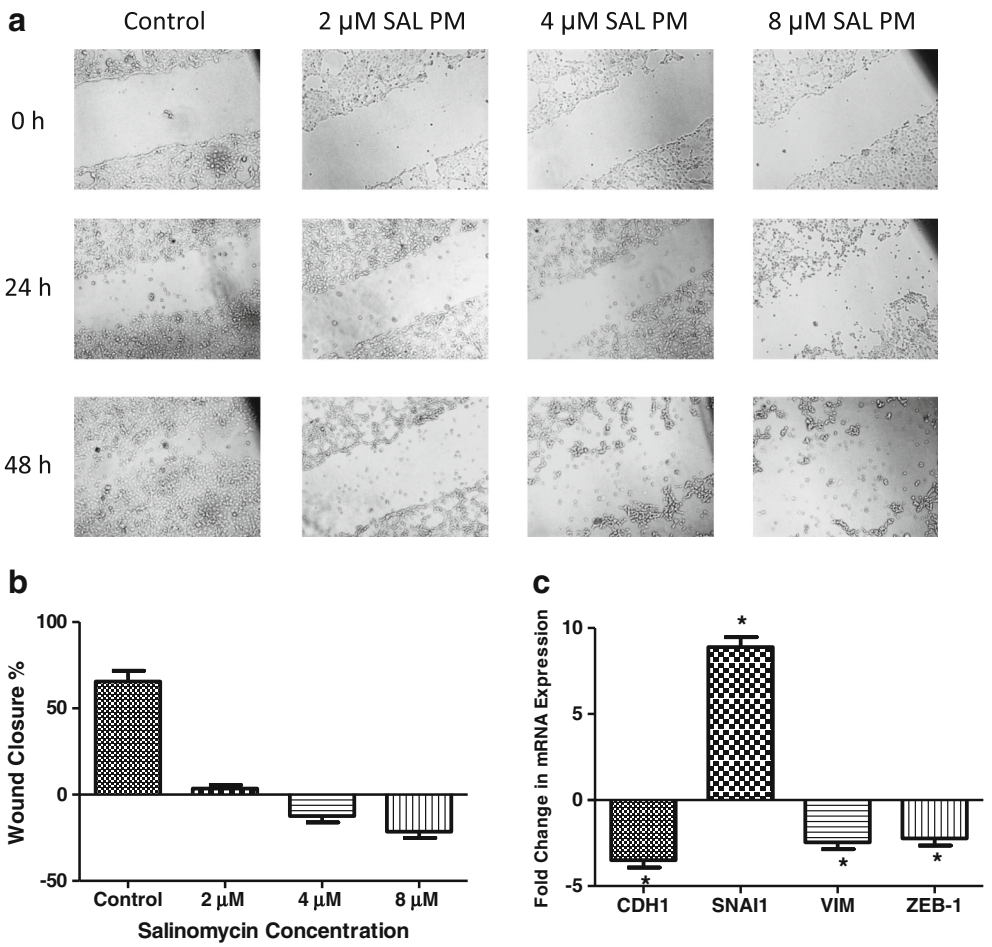

Fig. 4 (**a**) *In vitro* analysis of migration activity in AsPC-1 cells after 24 and 48 h treatment with SAL-loaded polymeric micelles (**b**) closure rate of scratch-wounded cultures of control and SAL treated AsPC-1 cells at 48 h post wounding (**c**) Changes in EMT-associated genes in AsPC-1 cells subjected to $IC_{50\%}$ dose of SAL-loaded PEG-b-PLA micelles for 48 h, * indicates $P < 0.001$, compared with untreated cells.

DISCUSSION

PC is one of the most incurable malignant tumors, with majority of patients diagnosed at metastatic stage of the disease (20). Although adjuvant gemcitabine-based chemotherapies are promising treatments for extending the survival rate after surgery, the clinical outcome is quite inefficient by the issues of its rapid metabolic inactivation, narrow therapeutic window, and dose-related toxicities (4). Moreover, the intrinsic or extrinsic resistance to gemcitabine remains an unsolved problem that hinders gemcitabine-based treatments. The inherent tumor resistance to gemcitabine has been linked to different mechanisms such as expression of EMT phenotype in cancer cells (21).

In this contribution, we used SAL as a new anticancer drug for delivery to gemcitabine-resistant PC model. However, the poor solubility of this active compound is the main obstacle for development of a clinically useful pharmaceutical formulation of it. Besides, the severe side effects of many anticancer drugs including SAL have limited their clinical applications due to their non-selective targeting of normal cells. In this regard, PM offer various advantages in oncology such as solubilization of hydrophobic drugs in their inner core, long circulation, and passive targeting of anticancer drugs to the tumor site (14). The PEG-PLA copolymer, which is nontoxic and not accumulative in the body at low concentrations, was selected as the building block of SAL micellar carrier because of its superior performance as a delivery system for paclitaxel in Genexol-PM formulation (15). Moreover, its low critical micelle concentration (CMC≈4 μg/mL) makes the PEG-PLA micelles to be potentially stable against dilution in the blood after systemic injection (17). Regarding the blood volume of 58.5 mL per kg of body weight of a mouse (22), and the injected dose of PEG-PLA (1.5 mg), we estimated the blood concentration of the copolymer to be approximately 850 μg/mL which was more than 200 times higher than its CMC. Moreover, our group had previously examined the physical stability of this micellar system in 10% fetal bovine serum in PBS and the results had shown acceptable stability of PEG-PLA micelles in this medium (17).

In order to make advantage out of enhanced permeability and retention (EPR) effect, the size of nanoparticulate drug delivery systems should be less than 200 nm (23). In this study, 10% *w/w* SAL-loaded PEG-PLA micelles which were prepared by nanoprecipitation technique, was found to be 154.5 ± 10.6 nm with narrow size distribution (PDI = 0.22).

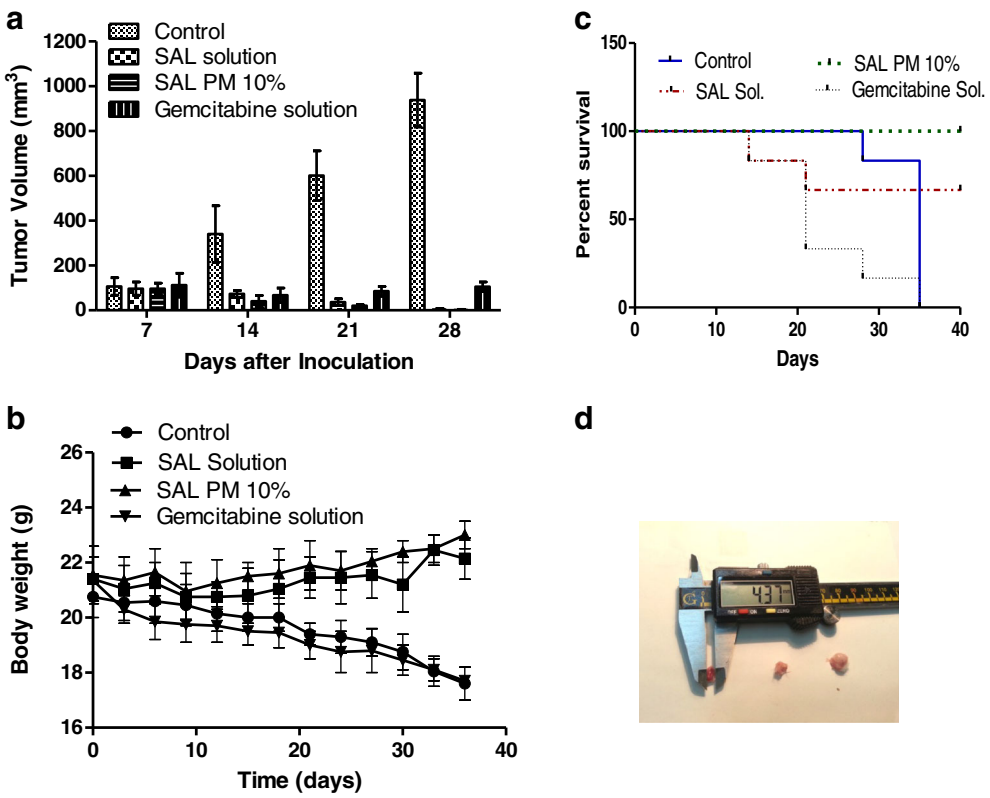

Fig. 5 *In vivo* antitumor efficacy of free and micellar SAL compared to that of gemcitabine solution and control groups determined in PC xenograft bearing Balb/c mice (**a**) mean tumor volume (mm^3) (**b**) mean body weight of mice (g) (**c**) Kaplan–Meier survival curve (**d**) photographs of tumor tissues after 7 days post inoculation.

In this regard, the fabrication method showed significant impact on the size of final PMs.

The results from *in vitro* SAL release in PBS (pH = 7.4) containing 0.5% SDS demonstrated a biphasic pattern. The burst release phase is usually caused by quick diffusion of drugs adsorbed onto the surface of NPs, while the controlled release phase depends on diffusion and/or erosion mechanisms. The slow release pattern of SAL shows that the PEG-PLA micelles were able to retain the incorporated drug. It seems that the high affinity between drug molecules and the hydrophobic core of PMs is responsible for the slow phase (24).

We had previously shown that the human PC AsPC-1 cells were highly resistant to gemcitabine, with more than 70% viability after treatment with 100 μM drug concentration (17). Yet, using SAL in either free form or encapsulated in PMs led to low survival rates of these cells. *In vitro* SAL cytotoxicity study also showed almost similar $IC_{50\%}$ values on normal NIH3T3 fibroblast cells. Fibroblasts are the main cellular component of the extracellular matrix of tumors, which notably hampers NPs penetration into tumor cells (25). Hence, it seems that SAL is potentially capable of targeting the non-neoplastic cells within the tumor microenvironment, which is a promising opportunity toward more efficient cancer therapy.

After treatment, AsPC-1 cell apoptosis was investigated using FITC-Annexin V/PI staining. Annexin V is commonly used as a probe to label phosphatidylserine during its apoptosis-associated externalization (26). Results indicated that SAL-loaded PMs could induce significant apoptosis on these PC cells, in accordance with previous findings on free SAL solution (27).

We also sought to determine the specific effects of SAL-loaded PMs on CSC traits, EMT phenotype and invasiveness within PC AsPC-1 cells. CD133 is a well-documented PC stem cell marker (28). Previous reports had shown a selective targeting of CD133+ cells by SAL treatment (12,29). However, using the $IC_{50\%}$ of SAL-loaded PMs, our data revealed that CD133+ cells were killed in the same rate as normal cancer cells indicating that the PC stem cells were neither resistant nor superiorly sensitive to SAL treatment while many conventional anticancer agents lead to enrichment of CSCs (7). The scratch wound healing assay showed that significant migration inhibition occurred at low drug concentration, whereas minor cell death was observed. Thus, it seems that SAL can inhibit the migration ability of AsPC-1 cells before it exerts any significant cytotoxic effect. On the other hand, EMT is a complex differentiation process during cancer invasion and metastasis in which expression of 4000 genes are transcriptionally changed (30). To find out whether SAL can influence signaling pathways involved in EMT, we measured the expression level of mRNA of four major genes in these signaling cascades. Contrary to our initial expectations, CDH1 and Snail were down- and up-regulated

respectively over a treatment period of 48 h with SAL-loaded PMs. This is in agreement with the known role of Snail as the repressor of the transcription of the CDH1 gene (31), but is in contrast to less degree of plasticity observed in scratch migration assay. The data showed that ZEB1 expression, a negative regulator of CDH1 and inducer of EMT (32,33), was reduced significantly following treatment, suggesting SAL as a suppressor of metastasis *via* inhibiting EMT. Snail priority over ZEB1 in regulating CDH1, aside from its expression level, can be a reflection of hierarchy between these proteins during EMT. Snail seems to recognize the recognition elements with higher affinity and resultantly can override ZEB1 in modulating CDH1 (34). Vimentin expression, another EMT marker, was also decreased in SAL PM treated cells which is in favor of chemotherapy sensitizing (35), disturbed cell migration and metastasis (36), and also better prognosis in gastric cancers (37). Furthermore, vimentin downregulation justifies impaired migratory ability of the treated cells in scratch migration assay and is in parallel with previous *in vivo* wound healing study (38). Collectively, it is clear that SAL harnesses EMT but through pathways which do not necessarily correspond to stem cells phenotype, something which has been demonstrated in previous studies as well (39,40).

Finally, the *in vivo* antitumor activity of SAL-loaded PEG-PLA micelles was evaluated in Balb/c mice with the subcutaneous PC model. Our data showed that despite the high dose of gemcitabine solution could significantly inhibit the tumor growth; this activity was accompanied by lower median survival time compared to the control group as well as significant body weight loss during the treatment period. In fact, the hydrophilic nature of this small molecule makes it prone to rapid distribution to other tissues than the tumor and quick elimination from the blood after injection (4). However, data in Fig. 5 showed that SAL was quite effective in not only inhibiting the tumor growth, but also reducing the tumor size. In this regard, both free SAL solution in 10% ethanol, and SAL embedded in PEG-PLA micelles were equally effective in demonstrating the antitumor activity ($p > 0.05$), a result consistent with previous reports that were obtained by using SAL-loaded iTEP NPs in orthotopic breast tumors or PEG-b-PCL PMs in xenograft model of breast cancer (13,41). However, the higher survival probability of mice treated with SAL-loaded PMs than the free SAL solution group, and the feasibility of PEG-PLA micelles to passive/active drug targeting to the tumor site, makes the current micellar drug delivery system highly promising for future therapeutic applications.

CONCLUSION

In the present study, we constructed and characterized a PM formulation of SAL that improved its solubility and *in vivo* antitumor activity compared to conventional gemcitabine monotherapy in PC. The ~10% drug loaded PMs showed spherical shape with particle size of 154.5 ± 10.6 nm and narrow size distribution, which could effectively retard the drug release kinetics. Due to its favorable pharmaceutical properties, the SAL-loaded PEG-PLA micelles achieved the longest survival in mice bearing PC xenografts. More importantly, the enhanced effect of SAL-loaded PMs was accompanied by induction of apoptosis in pancreatic AsPC-1 cells while inhibiting both cancer cells and CSCs proliferation and invasion. However, SAL's effect on inhibiting mesenchymal transition is obscure, which underlines the need for more complete understanding of its mechanism of action before any translation into clinics.

ACKNOWLEDGMENTS AND DISCLOSURES

We would like to express our profound thanks to Dr. Babak Paknejad for his assistance in animal experiments. This work is a part of the PhD project of first author and was financially supported by a grant numbered 91-03-33-19300 from Tehran University of Medical Sciences and Health Services.

REFERENCES

1. Holly EA, Chaliha I, Bracci PM, Gautam M. Signs and symptoms of pancreatic cancer: a population-based case–control study in the San Francisco Bay area. Clin Gastroenterol Hepatol. 2004;2(6):510–7.
2. Siegel R, Naishadham D, Jemal A. Cancer statistics, 2012. CA Cancer J Clin. 2012;62(1):10–29.
3. Heinemann V. Gemcitabine: progress in the treatment of pancreatic cancer. Oncology. 2000;60(1):8–18.
4. Brusa P, Immordino ML, Rocco F, Cattel L. Antitumor activity and pharmacokinetics of liposomes containing lipophilic gemcitabine prodrugs. Anticancer Res. 2007;27(1A):195–9.
5. Hung SW, Mody HR, Govindarajan R. Overcoming nucleoside analog chemoresistance of pancreatic cancer: a therapeutic challenge. Cancer Lett. 2012;320(2):138–49.
6. Shackleton M, Quintana E, Fearon ER, Morrison SJ. Heterogeneity in cancer: cancer stem cells versus clonal evolution. Cell. 2009;138(5):822–9.
7. Li Y, Kong D, Ahmad A, Bao B, Sarkar FH. Pancreatic cancer stem cells: emerging target for designing novel therapy. Cancer Lett. 2013;338(1):94–100.
8. Javle M, Gibbs J, Iwata K, Pak Y, Rutledge P, Yu J, *et al.* Epithelial-mesenchymal transition (EMT) and activated extracellular signal-regulated kinase (p-Erk) in surgically resected pancreatic cancer. Ann Surg Oncol. 2007;14(12):3527–33.
9. Singh A, Settleman J. EMT, cancer stem cells and drug resistance: an emerging axis of evil in the war on cancer. Oncogene. 2010;29(34):4741–51.
10. Gupta PB, Onder TT, Jiang G, Tao K, Kuperwasser C, Weinberg RA, *et al.* Identification of selective inhibitors of cancer stem cells by high-throughput screening. Cell. 2009;138(4):645–59.
11. Naujokat C, Steinhart R. Salinomycin as a drug for targeting human cancer stem cells. BioMed Res. Int. 2012;2012.

12. Zhang G-N, Liang Y, Zhou L-J, Chen S-P, Chen G, Zhang T-P, *et al.* Combination of salinomycin and gemcitabine eliminates pancreatic cancer cells. Cancer Lett. 2011;313(2):137–44.
13. Zhao P, Dong S, Bhattacharyya J, Chen M. iTEP nanoparticle-delivered salinomycin displays an enhanced toxicity to cancer stem cells in orthotopic breast tumors. Mol Pharm. 2014;11(8):2703–12.
14. Torchilin VP. Micellar nanocarriers: pharmaceutical perspectives. Pharm Res. 2007;24(1):1–16.
15. Lee KS, Chung HC, Im SA, Park YH, Kim CS, Kim S-B, *et al.* Multicenter phase II trial of Genexol-PM, a Cremophor-free, polymeric micelle formulation of paclitaxel, in patients with metastatic breast cancer. Breast Cancer Res Treat. 2008;108(2):241–50.
16. Kim SC, Kim DW, Shim YH, Bang JS, Oh HS, Kim SW, *et al.* In vivo evaluation of polymeric micellar paclitaxel formulation: toxicity and efficacy. J Control Release. 2001;72(1):191–202.
17. Daman Z, Ostad S, Amini M, Gilani K. Preparation, optimization and< i> in</i>< i> vitro</i> characterization of stearoyl-gemcitabine polymeric micelles: a comparison with its self-assembled nanoparticles. Int J Pharm. 2014;468(1):142–51.
18. Guglielmo Dusi VG. Liquid chromatography with ultraviolet detection of lasalocid, monensin, salinomycin and narasin in poultry feeds using pre-column derivatization. J Chromatogr A. 1999;835(1–2):243–6.
19. Pfaffl MW, Horgan GW, Dempfle L. Relative expression software tool (REST) for group-wise comparison and statistical analysis of relative expression results in real-time PCR. Nucleic Acids Res. 2002;30(9):e36. Comparative Study.
20. Stathis A, Moore MJ. Advanced pancreatic carcinoma: current treatment and future challenges. Nat Rev Clin Oncol. 2010;7(3):163–72.
21. Arumugam T, Ramachandran V, Fournier KF, Wang H, Marquis L, Abbruzzese JL, *et al.* Epithelial to mesenchymal transition contributes to drug resistance in pancreatic cancer. Cancer Res. 2009;69(14):5820–8.
22. National Centre for the Replacement Refinement & Reduction of Animals in Research. Mouse: Decision tree for blood sampling. 2014. Available from: http://www.nc3rs.org.uk/mouse-decision-tree-blood-sampling.
23. Greish K. Enhanced permeability and retention (EPR) effect for anticancer nanomedicine drug targeting. Cancer Nanotechnology: Springer; 2010. p. 25–37.
24. Rijcken C, Soga O, Hennink W, Van Nostrum C. Triggered destabilisation of polymeric micelles and vesicles by changing polymers polarity: an attractive tool for drug delivery. J Control Release. 2007;120(3):131–48.
25. Zhang J, Liu J. Tumor stroma as targets for cancer therapy. Pharmacol Ther. 2013;137(2):200–15.
26. Vermes I, Haanen C, Steffens-Nakken H, Reutellingsperger C. A novel assay for apoptosis flow cytometric detection of phosphatidylserine expression on early apoptotic cells using fluorescein labelled annexin V. J Immunol Methods. 1995;184(1):39–51.
27. He L, Wang F, Dai W-Q, Wu D, Lin C-L, Wu S-M, *et al.* Mechanism of action of salinomycin on growth and migration in pancreatic cancer cell lines. Pancreatology. 2013;13(1):72–8.
28. Olempska M, Eisenach PA, Ammerpohl O, Ungefroren H, Fandrich F, Kalthoff H. Detection of tumor stem cell markers in pancreatic carcinoma cell lines. Hepatobiliary Pancreat Dis Int. 2007;6(1):92–7.
29. Dong T-T, Zhou H-M, Wang L-L, Feng B, Lv B, Zheng M-H. Salinomycin selectively targets 'CD133+' cell subpopulations and decreases malignant traits in colorectal cancer lines. Ann Surg Oncol. 2011;18(6):1797–804.
30. Zavadil J, Bitzer M, Liang D, Yang Y-C, Massimi A, Kneitz S, *et al.* Genetic programs of epithelial cell plasticity directed by transforming growth factor-β. Proc Natl Acad Sci. 2001;98(12):6686–91.
31. Batlle E, Sancho E, Francí C, Domínguez D, Monfar M, Baulida J, *et al.* The transcription factor snail is a repressor of E-cadherin gene expression in epithelial tumour cells. Nat Cell Biol. 2000;2(2):84–9.
32. Eger A, Aigner K, Sonderegger S, Dampier B, Oehler S, Schreiber M, *et al.* DeltaEF1 is a transcriptional repressor of E-cadherin and regulates epithelial plasticity in breast cancer cells. Oncogene. 2005;24(14):2375–85.
33. Comijn J, Berx G, Vermassen P, Verschueren K, van Grunsven L, Bruyneel E, *et al.* The two-handed E box binding zinc finger protein SIP1 downregulates E-cadherin and induces invasion. Mol Cell. 2001;7(6):1267–78.
34. Bolós V, Peinado H, Pérez-Moreno MA, Fraga MF, Esteller M, Cano A. The transcription factor Slug represses E-cadherin expression and induces epithelial to mesenchymal transitions: a comparison with Snail and E47 repressors. J Cell Sci. 2003;116(3):499–511.
35. Du Z, Qin R, Wei C, Wang M, Shi C, Tian R, *et al.* Pancreatic cancer cells resistant to chemoradiotherapy rich in "stem-cell-like" tumor cells. Dig Dis Sci. 2011;56(3):741–50.
36. Ivaska J, Pallari H-M, Nevo J, Eriksson JE. Novel functions of vimentin in cell adhesion, migration, and signaling. Exp Cell Res. 2007;313(10):2050–62.
37. Fuyuhiro Y, Yashiro M, Noda S, Kashiwagi S, Matsuoka J, Doi Y, *et al.* Clinical significance of vimentin-positive gastric cancer cells. Anticancer Res. 2010;30(12):5239–43.
38. Eckes B, Colucci-Guyon E, Smola H, Nodder S, Babinet C, Krieg T, *et al.* Impaired wound healing in embryonic and adult mice lacking vimentin. J Cell Sci. 2000;113(13):2455–62.
39. Bae K-M, Su Z, Frye C, McClellan S, Allan RW, Andrejewski JT, *et al.* Expression of pluripotent stem cell reprogramming factors by prostate tumor initiating cells. J Urol. 2010;183(5):2045–53.
40. Kuo SZ, Blair KJ, Rahimy E, Kiang A, Abhold E, Fan J-B, *et al.* Salinomycin induces cell death and differentiation in head and neck squamous cell carcinoma stem cells despite activation of epithelial-mesenchymal transition and Akt. BMC Cancer. 2012;12(1):556.
41. Zhang Y, Zhang H, Wang X, Wang J, Zhang X, Zhang Q. The eradication of breast cancer and cancer stem cells using octreotide modified paclitaxel active targeting micelles and salinomycin passive targeting micelles. Biomaterials. 2012;33(2):679–91.